From Basic Network Principles to Neural Architecture: Emergence of Spatial-Opponent Cells

Ralph Linsker

PNAS 1986;83;7508-7512
doi:10.1073/pnas.83.19.7508

Proc. Natl. Acad. Sci. USA
Vol. 83, pp. 7508–7512, October 1986
Neurobiology

From basic network principles to neural architecture: Emergence of spatial-opponent cells

(modular self-adaptive networks/visual system/feature-analyzing cells)

RALPH LINSKER

IBM Thomas J. Watson Research Center, Yorktown Heights, NY 10598

Communicated by Richard L. Garwin, June 3, 1986

ABSTRACT **The functional architecture of mammalian visual cortex has been elucidated in impressive detail by experimental work of the past 20–25 years. The origin of many of the salient features of this architecture, however, has remained unexplained. This paper is the first of three (the others will appear in subsequent issues of these *Proceedings*) that address the origin and organization of feature-analyzing (spatial-opponent and orientation-selective) cells in simple systems governed by biologically plausible development rules. I analyze the progressive maturation of a system composed of a few layers of cells, with connections that develop according to a simple set of rules (including Hebb-type modification). To understand the prenatal origin of orientation-selective cells in certain primates, I consider the case in which there is no external input, with the first layer exhibiting random spontaneous electrical activity. No orientation preference is specified to the system at any stage, and none of the basic developmental rules is specific to visual processing. Here I introduce the theory of "modular self-adaptive networks," of which this system is an example, and explicitly demonstrate the emergence of a layer of spatial-opponent cells. This sets the stage for the emergence, in succeeding layers, of an orientation-selective cell population.**

A complex functional architecture for mammalian primary visual cortex (and precortical structures) has been experimentally elucidated over the past 20–25 years, spearheaded by the work of Hubel and Wiesel (1, 2). How complex do the rules that specify the development of this architecture need to be, and what are the organizing principles for this specification?

I have found that a surprisingly simple set of physiologically and anatomically plausible rules suffices to generate many of the salient features of this functional architecture. The starting point is a network comprising several two-dimensional layers of cells, with connections of unspecified strength to each cell of one layer from a neighborhood of cells of the preceding layer, and with a given rule for updating connection strength. The synaptic connection strengths reach their mature values under the influence of this rule, which in the present work is of Hebb type (3). This is a particular example of the class of systems that we shall call "modular self-adaptive networks." This means that the network arrangement is specified at the module (in this case, layer) level (e.g., "layer A provides input to layer B") and that a small amount of statistical information about the cell-to-cell connections is provided (e.g., the initial ratio of the numbers of excitatory and inhibitory synapses) but that the detailed connections and their strengths are unspecified and allowed to emerge during the development of the system.

The publication costs of this article were defrayed in part by page charge payment. This article must therefore be hereby marked "*advertisement*" in accordance with 18 U.S.C. §1734 solely to indicate this fact.

This paper shows how, and under what conditions, spatial-opponent cells (with central excitatory and peripheral inhibitory inputs at maturity, or with the reverse) emerge during the development of such a layered network, even in the absence of visual experience. The next paper in this series will show how orientation-selective cells (4) (which respond maximally to bars or edges of particular orientation) emerge in succeeding layers of the same system.

I emphasize that these papers deal with the emergence of network structure and differentiated cell types, starting with rules governing connection formation and modification. They do not address the biochemical and other mechanisms by which these lower-level rules may be implemented.

We are thus concerned with the following questions. Given some simple, biologically plausible rules for synaptic modification and for the basic structure of a network, and given only spontaneous electrical activity (no environmental input), do any biologically interesting network structures emerge? If they do, how constrained is the class of structures that can arise? If feature-analyzing cells of various types (e.g., opponent cells and orientation-selective cells) emerge, is their formation robust, or is it dependent upon precise choices of initial conditions and of modification rules?

We consider here a system having a simple gross architecture and development rule. This is in order to lay bare the mechanisms by which certain feature-analyzing functions observed in the visual system emerge even in a simply specified example of a modular self-adaptive network. More complicated assumptions—which may be appropriate if one's goal is a detailed model of a retinocortical pathway—may be analyzed using the same principles as are introduced here. As an example, a network of three layers—representing the photoreceptor, horizontal-cell, and bipolar populations—that has gross connectivity more complicated than the "A-to-B-to-C" arrangement we treat here could be used as a model for opponent-cell formation in the retinal bipolar layer.

SYSTEM SPECIFICATION

Fig. 1 shows the gross architecture of the system. Each cell of layer M (M = B or C) receives inputs from a large number of cells in an overlying region of the predecessor layer L. (Conversely, each L cell can supply input to a number of M cells.) The density of synapses from layer L to a given cell of layer M generally decreases as one proceeds away from the overlying point in any direction. Where a definite form is needed for calculation, we assume the synaptic distribution is Gaussian; i.e., has average density proportional to $\exp(-a^{M}r^{2})$. [The radius of this distribution is of order $r_M \equiv (a^{M})^{-1/2}$.] For simplicity, we consider each synapse to be located in layer L at some position that does not change during development. We refer to the set of all synaptic connections to a given postsynaptic cell as the arborization of the cell. Each synapse conveys as input to the postsynaptic M cell whatever "activity" value (next paragraph) is being generated by the L cell located at that synapse's position.

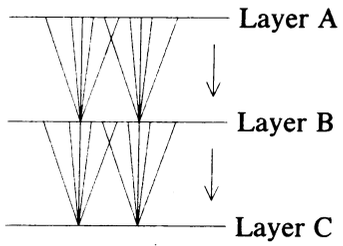

FIG. 1. Modular self-adaptive network diagram for the system discussed in this paper.

We characterize the signaling behavior of each cell, at any given time, by a number that we will call its "activity." (This can be thought of as corresponding to a spike frequency in the case of action potential-producing cells in biological systems.) A "presentation" π is defined as the set of activities $\{F^{L\pi}x\}$ at each location x in layer L at a given time.

We consider here the case in which there is no environmental input. We assume that the cells in layer A provide random spontaneous uncorrelated activity as input to layer B. For definiteness, think of A as divided into small boxes, each having sides of length δ, with activity $F^{A\pi}x$ being uniform within each box, uncorrelated between different boxes, and with no more than one or a few connections to a given B cell from any one box. For N_B synapses (from layer A to a given B cell) scattered over an area of order πr_B^2, this regime of interest is described by $N_B\delta^2/\pi r_B^2 \lesssim 1$. [The results are independent of whether the maximum number of connections from any A box to a given B cell is one (i.e., strict lack of any microcorrelation) or a few.]

We assume that, for each presentation, the output of a postsynaptic cell in layer M is a linear function of its inputs from layer L, with the input at the jth synapse being weighted by a "synaptic connection strength" c_j. That is,

$$F^{M\pi} = R_a + R_b\Sigma_j c_j F_j^{L\pi}, \qquad [1]$$

where $F_j^{L\pi}$ is the input activity seen by the jth synapse, and is equal to the layer-L activity $F^{L\pi}(x_j)$ at the position x_j of that synapse. R_a and R_b are taken to be constants ($R_b > 0$). In this notation the postsynaptic M cell is given no index. This should cause no confusion, since we shall be using Eqs. 1 and 2 to calculate the development of the connections from layer L to a single cell of layer M.

We take the view that the values of R_a, R_b, and the other constants we shall introduce are specified to be substantially the same for all cells of the same population—in this case, for all cells of the same layer M. In a biological system, these values would be specified either genetically or by earlier developmental processes that we are not considering here.

We use a Hebb-type rule for modifying connection strengths during development. We want $(\Delta c_i)^\pi$, the change in c_i due to presentation π, to be greater when the input activity $F_i^{L\pi}$ at the ith synapse is correlated with the output activity $F^{M\pi}$ of the postsynaptic cell and less when these activities are uncorrelated or anticorrelated. We choose a particularly simple form in which the change in c_i as a result of a presentation π is

$$(\Delta c_i)^\pi = k_a + k_b(F^{M\pi} - F_0^M)(F_i^{L\pi} - F_0^L), \qquad [2]$$

where k_a, k_b, F_0^M, and F_0^L are constants ($k_b > 0$). We assume that the connection strength changes very little with each presentation.

Hebb-type rules typically lead to connection strengths that increase or decrease without limit, unless some saturation condition is imposed. We will assume that each connection strength is bounded by two values: 0 and +1 for excitatory synapses and −1 and 0 for inhibitory synapses. All the features of interest also emerge if one makes the simpler, but biologically less reasonable, assumption that each connection strength has the same pair of limiting values (one negative, the other positive). Eq. 3, the ensemble-averaged form of Eq. 2, will accordingly be used except when c would thereby range beyond its allowed limits, in which case c will be held at its limiting value for that time step.

We assume that first the A-to-B connections, and then the B-to-C connections, develop to their mature values. In the next section we shall see that just four parameters per layer (which are functions of the constants introduced above) completely define the layer structure and the development process, apart from random variations (in synaptic position and initial c values).

METHODS

The Ensemble-Averaged Development Equation. Since we have assumed that the c values change very little with each presentation, we can average Eq. 2 over an ensemble of presentations, using Eq. 1 to express $F^{M\pi}$ in terms of the $\{F_j^{L\pi}\}$ values. This gives $\dot{c}_i$, the rate of change of c_i, averaged over a time long compared to each presentation, but short compared to the time required for layer maturation:

$$\dot{c}_i = k_1 + \frac{1}{N_M}\Sigma_j(Q_{ij}^L + k_2)c_j. \qquad [3]$$

Here

$$Q_{ij}^L \equiv f_0^{-2}\langle(F_i^{L\pi} - \overline{F}^L) \times (F_j^{L\pi} - \overline{F}^L)\rangle_\pi; \qquad [4]$$

angle brackets denote the ensemble average; $k_1 \equiv [k_a + k_b(R_a - F_0^M)(\overline{F}^L - F_0^L)]/(N_M k_b R_b f_0^2)$; $k_2 \equiv \overline{F}^L(\overline{F}^L - F_0^L)/f_0^2$; N_M is the total number of inputs to the M cell; f_0 is an arbitrary unit of activity (introduced to allow convenient normalization of Q_{ij}^L); the unit of time is defined for convenience so that the number of presentations per unit time [which enters $\dot{c}_i \equiv N_{pres}\langle(\Delta c_i)^\pi\rangle_\pi$] is $N_{pres} \equiv 1/(N_M k_b R_b f_0^2)$; and $\overline{F}^L$ is the ensemble-averaged activity at any point of layer L. The values of $\overline{F}^L$ and Q_{ii}^L are substantially independent of location, for the present system in the absence of external input. (For layers beyond the first, these values are subject to random variations resulting from layer nonuniformities, which we shall discuss, but there is no systematic positional bias in our system, as there could be if a biased ensemble of inputs were being presented to the network.)

The function Q_{ij}^L is proportional to the autocorrelation function of the activities at two points in layer L: the positions of synapses i and j that share the same postsynaptic M cell. This does not imply any direct interaction between the two synapses. The Q_{ij}^L function arises because the Hebb rule refers to the correlation between pre- and postsynaptic activities, and the postsynaptic output activity is a linear function of all the inputs.

The Program. To calculate the development of each layer M in turn, we do the following: (*i*) Calculate the Q^L function appropriate to an ensemble of random layer-A presentations, as processed by the mature intervening layers through and including layer L. (*ii*) For each set of parameter values, and for a postsynaptic M cell having synapses placed at random according to the specified density distribution, choose a random set of initial c values and solve Eq. 3 for the development of the M cell. The four parameters for each layer are k_1, k_2, $a^L/a^M(= r_M^2/r_L^2)$, and n_{EM}. In our simulations, a fraction n_{EM} of the L-to-M synapses have c limits 0 and 1, and the rest, −1 and 0; alternatively, all of the synapses have c limits $n_{EM} - 1$ and n_{EM}. (*iii*) Explore the sensitivity of the mature cell morphologies to the random initial choices. If the mature morphology is substantially independent of the ran-

dom choices (i.e., is determined by the four parameter values, which we take to be uniform for all M cells), then layer M will mature to be populated by cells of uniform morphology. If this insensitivity to random synaptic positions and initial c values is indeed the case, then return to step 1 to calculate Q^{M} and solve for the maturation of the next layer.

RESULTS

From the given set of specifications (which embody rather weak assumptions, none of which are specific to visual processing), we shall see that spatial-opponent cells emerge in layer C.

Tendency of Synaptic Connection Strengths (c) to Reach Limiting Values. Any mature cell (i.e., a cell for which all c have reached stable final values) in this system must have all, or all but one, of its c values "pinned" at limiting values. *Proof*: Suppose the opposite, and let c_1 and c_2 be intermediate c values satisfying $\dot{c}_1 = \dot{c}_2 = 0$. To check stability against small perturbations, let c_1 be increased by a small amount ε, and let c_2 be decreased by ε. Then the new value of $\dot{c}_1 = \varepsilon \times (Q^{L}_{11} - Q^{L}_{12})/N_M$, which is positive in the present system since the activity correlation of a cell with itself exceeds the correlation between two different cells. Similarly, the new value of $\dot{c}_2 = -\varepsilon \times (Q^{L}_{22} - Q^{L}_{21})/N_M$ is negative. Hence the system is unstable against this perturbation; the new values of $\dot{c}_{1,2}$ cause the perturbation to amplify, rather than causing the system to return to its unperturbed state. All of our mature cells obtained by simulation are found to have all (or all but one) c at limiting values.

Development of the A-to-B Connections. For random spontaneous activity in layer A, $Q^{A}_{ij} = 1$ if i and j lie in the same A box (defined above), and 0 otherwise. For each B cell, place N_B synapses randomly according to the distribution $\exp(-a^{B}r^2)$, choose random initial c_i values (from some distribution that may, but need not, be the same for all B cells), and solve Eq. 3. If $|k_1|$ and $|k_2|$ are both $\leq 1/N_B$, then each B-cell's development depends upon its initial c values. Suppose instead that $|k_1|$ and/or $|k_2| >> 1/N_B$. We define $\bar{k} \equiv -k_1/k_2$. Then there are four parameter regimes yielding different outcomes for layer-B maturation. The boundaries between the regimes are independent of random initial choices, except for small terms of order $1/N_B$.

The parameter regimes (presented below) can be derived analytically by making use of three facts. First, Eq. 3 shows that for $\dot{c}_i$ to be positive for some i and negative for others, $(k_1 + k_2 g)$ must be zero to within terms of order $1/N_B$, where $g \equiv (\Sigma c_j)/N_B$. Second, g has to lie between the extremes $n_{EB} - 1$ and n_{EB}. Finally, a mature cell having non-extreme g value can be stable only if $k_2 < 0$. Explicit simulation of B-cell development confirms the existence of four regimes. (*i*) $k_2 < 0$ and $\bar{k} > n_{EB}$, or $k_2 > 0$ and $\bar{k} < n_{EB} - 1$. All mature B cells are "all-excitatory"—i.e., all c values reach their excitatory limits. (As per the earlier discussion of c-"pinning," "all c values" should be read as "all or all but one per B cell.") (*ii*) $k_2 < 0$ and $\bar{k} < n_{EB} - 1$, or $k_2 > 0$ and $\bar{k} > n_{EB}$. All mature B cells are "all-inhibitory." (*iii*) $k_2 > 0$ and $n_{EB} - 1 < \bar{k} < n_{EB}$. If the initial value of g for a given B cell is less than (or greater than) $\bar{k}$, the cell will mature to become all-inhibitory (resp., all-excitatory). Uniformity of layer-B morphology in this regime is contingent upon substantially all initial g values lying on one side or the other of $\bar{k}$. (*iv*) $k_2 < 0$ and $n_{EB} - 1 < \bar{k} < n_{EB}$. The mature state will have $g = \bar{k}$ regardless of initial c values. The random initial c values will determine which subset of connections (for each B cell) mature to their excitatory c limits and which to their inhibitory limits. The arrangement of mature c values for any B cell is random; it exhibits no spatial structure (on a scale greater than δ). We say that each B cell is of "mixed" excitatory/inhibitory type.

To proceed further, we choose parameters in the regime such that all B cells are all-excitatory. (The same analysis applies to the case in which all B cells are all-inhibitory.)

In this system, all B cells have the same values of k_1, k_2, n_{EB}, and a^{B}. A useful treatment of cell-to-cell parameter fluctuations would involve specific assumptions about the mechanisms that generate particular parameter values; this is beyond the scope of the present discussion.

Activity Correlation in Mature Layer B. Consider two all-excitatory B cells n and m, separated by a distance s. Each cell has N_{EB} excitatory synaptic inputs, each with $c = 1$. Using Eq. 4 (with L = B) and Eq. 1, we find that Q^{B}_{nm} is proportional to the number of pairs of synapses i,j for which i and j share the same A box (where i is an input to n and j is an input to m). This value is well described (for the regime $N_{EB}\delta^2/\pi r_B^2 << 1$) by $Q^{B}_{nm} = Q^{B}_{mn} = (2\pi/\beta^2) \times \mathrm{BINOM}(N_{EB}, p)$. Here we define $\beta \equiv N_{EB}\delta/r_B$. BINOM is a random value selected from the binomial distribution whose parameters are N_{EB} and $p \equiv (\beta^2/2\pi N_{EB}) \times \overline{Q}^{B}(s)$, where the mean value of Q^{B}_{nm} (for given s) is $\overline{Q}^{B}(s) = \exp(-a^{B}s^2/2)$. [We choose the normalization $\overline{Q}^{B}(0) = 1$.] The random variation in Q^{B}_{nm} from one B-cell pair n,m ($n \neq m$) to another at fixed s is of order $(2\pi)^{1/2}/\beta$ for s near zero. The value of Q^{B}_{nn}, for any n, is approximately $2\pi N_{EB}/\beta^2$.

These results can be verified by explicitly generating an ensemble of random synaptic placements for given s. To see how the Gaussian form of $\overline{Q}^{B}(s)$ arises, note that in the continuum limit the overlap between two B cells is $\propto \int \exp(-a^{B}|x|^2) \times \exp(-a^{B}|x - s|^2)d^2x \propto \exp(-a^{B}|s|^2/2)$.

As an example, two nearby cells having $N_{EB} \simeq 1000$, $\delta \simeq 4$ μm, and $r_B \simeq 400$ μm (hence $\beta \simeq 10$) will have an average of $\beta^2/2\pi \simeq 16$ ($\pm$ 4) synaptic input locations (A boxes) in common, out of a total of 2000 inputs. The number of such common inputs (proportional to Q^{B}_{nm}) is the only spatial information (concerning the distance between n and m) available to the development Eq. 3.

How many presentations (in an ensemble) are needed to ensure that two cells n and m with no common inputs do not have—by chance—an ensemble-averaged activity correlation (see right-hand side of Eq. 4) that is comparable to that for nearby pairs of cells? (The strict rule that $Q^{A}_{ij} = 0$ unless i and j share an A box, which we use in our simulations, is only true for a sufficiently large ensemble.) The order-of-magnitude condition for the required ensemble size M is $N_{EB}(2/M)^{1/2} << \beta^2/2\pi$ or $M >> 8000$ for the numbers used above. If, say, ten presentations are generated per second, this means that the infinite-ensemble limit is a good approximation provided that c values do not change much over a 15-min interval.

From Layer B to C: The Emergence of Spatial-Opponent Cells. First we discuss a simulation with the random Q^{B}_{nm} variations included and show that opponent cells, whose morphology is insensitive to the random choices of initial c values and synaptic positions, emerge in layer C. Then we systematically study the parameter space for C-cell development, focusing on the large-β regime in which Q^{B}_{nm} can be approximated by $\overline{Q}^{B}(s)$.

For Q^{B}_{nm} ($n \neq m$), choose values from the binomial distribution appropriate to $\beta = 10$ (a large-variation case). (This distribution is essentially independent of whether $N_{EB} = 100$, 600, or 6000, as long as β is fixed.) To fix a value for $Q^{B}_{nn} \simeq 2\pi N_{EB}/\beta^2$, we choose $N_{EB} = 600$ (so $\delta/r_B = 1/60$).

We simulate the development of C cells each having $N_C = 600$ synaptic inputs (a practical computational value), with parameter values, $k_1 = 0.45$, $k_2 = -3$, $a^{B}/a^{C} = 3$ (i.e., $r_C/r_B = 3^{1/2}$). Each c value is limited to the interval -0.5 to $+0.5$, corresponding to $n_{EC} = 0.5$. (Using c limits of $n_{EC} - 1$ and n_{EC} for all synapses leads to the same cell morphology, apart from random variations, as is obtained using a fraction n_{EC} of excitatory synapses and a fraction $1 - n_{EC}$ of inhibitory

synapses with c limits of 0,1 and -1,0, respectively. The difference is a practical one: roughly half of the synapses mature to $c = 0$ in the latter case and hence do not contribute to the Q sum in Eq. 3. Hence the random variation in synaptic density seen by the development equation is greater, for given N_C, in the latter case than in the former. In the large-N_C limit, density fluctuations are small and this distinction vanishes.) We start with c values drawn either from the uniform distribution on the interval -0.5 to $+0.5$ (used for Fig. 2), or (to study biased initial conditions) uniform on the interval $-0.5,+0.1$ or $-0.1,+0.5$, or normal with mean = -0.2, SD = 0.05.

Fig. 2 shows a resulting mature C cell: an "ON-center" circularly symmetric opponent cell with a mature average c value of $g = 0.167$. Repeated runs with different initial c values, initial-c distributions, and synaptic positions give the same mature cell type and g value with essentially the same excitatory-core radius. The transition region (between core and surround, within which excitatory and inhibitory c values coexist) becomes sharp as the relative contribution of the self-term Q_{nn} (compared with the overall Q sum in Eq. 3) is reduced—for example, by increasing N_C to dilute the contribution of the self-term or by decreasing N_{EB} at fixed β.

The above simulations show that opponent cells form even when there are large random variations in the Q^B_{nm} values. Now we consider the low-variation (large-β) case.

We summarize our findings for a set of about 70 simulations using $\overline{Q}^B(s)$ in place of Q^B_{nm}. The use of $\overline{Q}^B(s)$ is valid in the limit where β is large [so that random variations in Q^B_{nm} ($n \neq m$) are small] and where the contribution of the self-term Q^B_{nn} does not dominate the Q sum (for N_C of order N_{EB}, this is also assured when β is large). In these runs, $|k_1|$ and/or $|k_2| > 0.04$, $-k_1/k_2$ ranges from < -0.5 to >0.5, and r_C/r_B ranges from $3^{-1/2}$ to $10^{1/2}$. We use $N_C = 300$ synapses for most of the runs ($N_C = 600$ for confirmatory runs) and set the limits for each c at $n_{EC} - 1$ and n_{EC}, where n_{EC} is typically 0.5 but ranges from 0.35 to 0.65.

The all-excitatory and all-inhibitory cell types (corresponding to g lying at its extreme values n_{EC} and $n_{EC} - 1$, respectively) emerge as they did in the development of the previous (B) layer. Now the Q term is no longer of order $1/N_M$, since for each synaptic input from a B cell n, many other inputs to the same C cell from B cells m (not just one or a few inputs, as in the A-to-B case) have $Q^B_{nm} \neq 0$. Therefore, the difference between g and $-k_1/k_2$ will not be as small as of order $1/N_M$, as it was for B-cell development. Nonetheless, when $|k_{1,2}|$ exceed several tenths, $-k_1/k_2$ predicts the mature g value to a good approximation (*cf.* $g = 0.167$ for $-k_1/k_2 = 0.15$ in the example of Fig. 2).

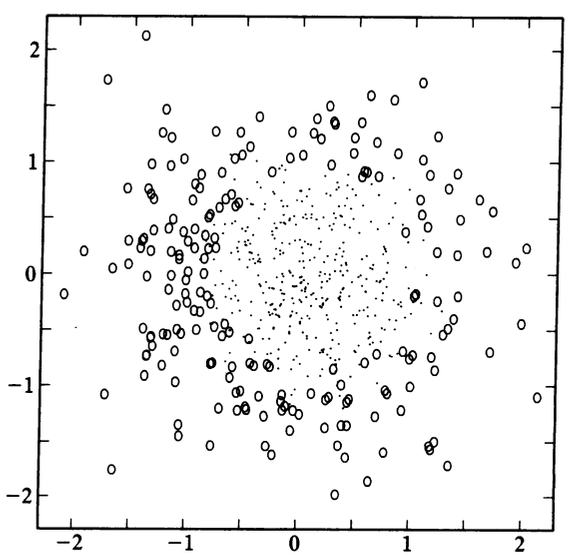

FIG. 2. Synaptic positions and mature connection strengths for a single cell of layer C having 600 synapses. Parameter values are $k_1 = 0.45$, $k_2 = -3$, $r_C/r_B = 3^{1/2}$, and each c value is allowed to range between -0.5 and $+0.5$. Random initial c values are chosen from uniform distribution on the interval -0.5 to $+0.5$. Values of Q^B_{nm} are appropriate to random placement of A-to-B and B-to-C synapses; layer uniformity is not assumed (see text). At maturity, every c reaches an extreme value: 0.5 (indicated by an oval) or -0.5 (dot). Axes are labeled by distance from cell center (in units of r_C).

For $k_2 < 0$, we pass through a series of regimes as k_1 is decreased. (*i*) Each cell all-excitatory. (*ii*) Each cell an "ON-center" circularly symmetric opponent cell (for g between approximately 0.15 and 0.5, when $n_{EC} = 0.5$). The transition between excitatory core and inhibitory surround is sharp (no intermingling), since the Q^B_{nn} self-term (which was included in the simulation for Fig. 2 and was relatively large there) is now replaced by $Q^B(0)$. The excitatory-core radius r_{core} for given g is given analytically (apart from random variations) by $\exp(-a^C r^2_{core}) = n_{EC} - g$. For the case ($N_C = 300$, $n_{EC} = 0.5$, $k_1 = 0.45$, $k_2 = -3$, $a^B/a^C = 3$), 10 out of 10 trials (with different random initial conditions) yield the "ON-center" mature morphology with g ranging between 0.164 and 0.168. How regular is the morphology from cell to cell? The core is centered to within a standard deviation of $0.04r_C$ along each axis (this is the position of the cell's centroid, calculated by weighting each synapse's position by its mature c value). The core radius (defined here as the radius of the cell-centered circle that encloses the maximum value of Σc_i) is $r_{core}/r_C = 1.06 \pm 0.06$, compared with the value of 1.10 found analytically (see above) for a perfectly symmetric cell of this g value.

(*iii*) As we continue to lower k_1 (so that g lies approximately in the range -0.1 to $+0.1$, for $n_{EC} = 0.5$), the mature core becomes eccentric and then "breaks through" to the periphery, so that the excitatory/inhibitory boundary is an arc or a straight line passing through the cell's center (when $g \simeq 0$). For the case ($N_C = 300$, $n_{EC} = 0.5$, $k_1 = 0$, $k_2 = -3$, $a^B/a^C = 3$), 10 runs yielded 3 cells with essentially straight boundaries (through the center), 6 with arced boundaries, and 1 with an eccentric enclosed excitatory region. The orientation of these mature, rotationally asymmetric cells varies randomly from cell to cell.

As k_1 is made more negative, we reach (*iv*) an "OFF-center" (centrally inhibitory, peripherally excitatory) circularly symmetric opponent-cell regime, and finally (*v*) an all-inhibitory regime. Note that Eq. 3 is unchanged when the sign of k_1 and the role of excitatory and inhibitory c values are both reversed.

DISCUSSION

For a multilayer network with local feedforward connections that develops, one layer at a time, under the influence of a Hebb-type synaptic modification rule, I have found (*i*) that the developmental options for each of the first two stages of connections (A-to-B and B-to-C) are relatively constrained; (*ii*) that (over a wide range of parameter values) the mature cell morphology depends only upon the values of a few parameters that are specified for the entire layer, is independent of random cell-to-cell variations in synaptic position and initial c values, and hence is uniform over the newly matured layer; and (*iii*) that spatial opponency appears as a morphologic option, for the first time, in the third layer C. Opponent cells emerge in the absence of environmental input if spontaneous random electrical activity is assumed in the first layer. None of these assumptions is specific to visual processing. Although a Hebb-type rule has been used here, I do not suggest that a rule of this type is required for the emergence of the demonstrated cell types.

In this system, random input is progressively structured by each layer of connections (as it matures in its turn). The development of all-excitatory (or all-inhibitory) cells in layer B induces spatial correlation of layer-B activity (on the scale of the arborization breadth), which was not present in layer A. This enables the center–surround opponent-cell morphology to develop in layer C. In contrast, no segregation into excitatory and inhibitory regions is possible during layer-B maturation, even though the identical development rule applies to both layers.

Depending upon the parameter regime, layer C can develop as a uniform layer of circularly symmetric opponent cells or of all-excitatory or all-inhibitory cells. There is an additional regime in which the mature C cells are rotationally asymmetric and hence display orientation selectivity. For cells with 300–600 synapses, I have found the cell-to-cell variability (of mature morphology) in this regime to be substantially greater than in the circularly symmetric opponent-cell regime. The detailed study of the variability of this orientation-selective layer-C morphology as a function of synaptic number (and other factors such as random Q^{B}_{nm} variations) is beyond the scope of this paper.

Some interesting, though very approximate, signal-to-noise relationships between neuronal "device properties" (N_M and δ/r_B), the size of the presentation ensemble, and system development have arisen during this work. These relationships appear well satisfied for biologically plausible choices of these values.

Maturation Process for a Layer-C Opponent Cell. To understand how an "ON-center" opponent cell forms, rather than just studying the final state, let us consider the maturation sequence for a cell in this regime, having positive k_1, negative k_2, and initial average c near 0. (The cell of Fig. 2 is representative). (*i*) The positive k_1 causes all c to increase, making the locally averaged c values positive. (*ii*) Now, since synaptic density is greater centrally than peripherally, the sum over synapses causes the contribution of the Q^{B} term in Eq. **3** to be greater when the synapse being modified is central than when it is peripheral. This causes the central region to saturate first and become excitatory. (*iii*) The negative k_2 then causes the peripheral c values to decrease (since negative k_2 favors Σc_j to be near zero) and eventually saturate at the inhibitory limit. (If k_2 were less negative, or were positive, the periphery would become excitatory as well, leading to an all-excitatory solution.)

For this and more general Hebb-type rules, the following heuristic argument explains why the opponent-cell morphology emerges. Let P_0 be the likelihood that the input activity I_i at the ith synapse of a given M cell is "high." Let $P_{c,i}$ be the conditional likelihood that I_i is "high" given that the postsynaptic output O is "high." Assume each input makes only a small contribution to O. For a peripheral synapse, $P_{c,i}$ will be close to P_0 in value—the output hardly "cares" whether the ith input is low or high. But for a central synapse, I_i is correlated with the input activities at many neighboring synapses (because the synapses are centrally more dense.) Therefore, central $P_{c,i}$ will be significantly greater (or less) than P_0 if the locally-averaged c value is positive (resp., negative). A Hebb-type rule will therefore increase the central more than the peripheral c values (if the locally averaged c is positive), since there is a greater correlation between synaptic input and postsynaptic cell response for the central synapses. What is crucial here is the difference between central and peripheral $P_{c,i}$. The results are similar whether this difference is caused by a synaptic density gradient, as here, or by some other factor (e.g., dendritic cable properties).

Context of This Work. The developmental stages described in this paper do not represent an attempt to model the retina. For example, horizontal and amacrine cells are not included, and nonspiking retinal cells and spiking (action potential-producing) cells are not treated differently. Rather, the purpose of this paper and the two to appear later is to see whether a simple modular self-adaptive network generates structures that are found in real biological systems, as a guide to exploring how ubiquitous these features of neural architecture may be, and how a few basic network-modification rules can induce system-level structures and behaviors of biological importance.

1. Hubel, D. H. & Wiesel, T. N. (1977) *Proc. R. Soc. London Ser. B* **198**, 1–59.
2. Fregnac, Y. & Imbert, M. (1984) *Physiol. Rev.* **64**, 325–434.
3. Hebb, D. O. (1949) *The Organization of Behavior* (Wiley, New York).
4. Wiesel, T. N. & Hubel, D. H. (1974) *J. Comp. Neurol.* **158**, 307–318.